Speech Driven Video Editing via an Audio-Conditioned Diffusion Model

Dan Bigioi
University of Galway
d.bigioi1@nuigalway.ie

Shubhajit Basak*
University of Galway
s.basak1@nuigalway.ie

Michał Stypułkowski*
University of Wrocław
michal.stypulkowski@cs.uni.wroc.pl

Maciej Zięba
Wrocław University of Science and Technology
Tooploox
maciej.zieba@pwr.edu.pl

Hugh Jordan
Trinity College Dublin
jordanhu@tcd.ie

Rachel McDonnell
Trinity College Dublin
ramcdonn@tcd.ie

Peter Corcoran
University of Galway
peter.corcoran@universityofgalway.ie

Abstract

Taking inspiration from recent developments in visual generative tasks using diffusion models, we propose a method for end-to-end speech-driven video editing using a denoising diffusion model. Given a video of a talking person, and a separate auditory speech recording, the lip and jaw motions are re-synchronized without relying on intermediate structural representations such as facial landmarks or a 3D face model. We show this is possible by conditioning a denoising diffusion model on audio mel spectral features to generate synchronised facial motion. Proof of concept results are demonstrated on both single-speaker and multi-speaker video editing, providing a baseline model on the CREMA-D audiovisual data set. To the best of our knowledge, this is the first work to demonstrate and validate the feasibility of applying end-to-end denoising diffusion models to the task of audio-driven video editing. [1]

1. Introduction

The idea behind audio-driven video editing is to provide a means to re-synchronise the lip and jaw movements of an actor in a video, in response to a new speech input signal. This new speech signal may come from the original speaker, or a voice actor. Regardless of the source of the input speech, a key objective is that the performance of the actor is never diminished. No matter how the lip and jaw movements change in response to the new audio, the facial expressions, and emotions portrayed by the actor should remain consistent with the original performance.

Achieving such seamless audio-driven video editing is an exciting prospect for the entertainment industry, one with the potential of being applied to movies, TV shows, live streaming, and even homemade content uploaded to platforms such as YouTube, TikTok, and others. Giving video content creators the ability and option to edit their work without having to go through time-consuming, and expensive re-shoots, allows them to work with a greater tolerance for error during filming.

Furthermore, the realisation of true audio-driven video editing would bring about a significant transformation in the world of cinema and television, allowing for more accessible and cost-effective dubbing of English-language movies/TV shows/videos into other languages and vice versa, allowing for the further democratisation of video content by making it more engaging and personalized for audiences worldwide. Recent advancements in deep learning and talking head generation techniques are bringing us closer to this exciting possibility, where audio and video will be seamlessly synchronized in real-time.

Current approaches for speech driven video editing, and the related task of talking head generation can be grouped into two distinct types: structured, and unstructured. Structured generation refers to techniques that use the speech signal to first extract an intermediate structural representation of the face (facial landmarks, 3D model expression parameters), before utilizing it to render the photo-realistic frame [7, 31, 70, 85, 88]. On the other hand, unstructured generation techniques [18, 29, 72, 87], utilise image reconstruction techniques to generate the photo-realistic frame

*Both Authors Contributed Equally to the Paper

[1] All code, datasets, and models used as part of this work are made publicly available here: https://danbigioi.github.io/DiffusionVideoEditing/

directly in an end-to-end manner.

Diffusion models [16, 24, 48, 61] are a relatively new class of generative model that have recently been gaining traction due to their strong performance on image synthesis tasks, often outperforming state-of-the-art GAN (Generative Adversarial Network) [20]-based methods [16]. Utilising conditioning signals such as text and even images, diffusion models have shown that they can be trained and conditioned towards generating a specific desired output at inference time with relative ease [55]. They achieve high mode coverage unlike GANs, maintain high sample quality, and are stable during training. These properties make them an ideal candidate for application towards the task of unstructured audio-driven video editing, a task that has thus far been dominated by GAN-based approaches [8, 11, 72].

We present an approach for automatic speech driven video editing using a denoising diffusion model. We utilise a U-Net backbone modifying it for the task of video editing, and introduce a feature concatenation mechanism for conditioning the network with information related to the previously generated frame in the sequence so that the network can generate temporally coherent frames. We further condition the network on speech by feeding spectrogram feature embeddings combined with the noise signal throughout the residual layers of the U-Net as demonstrated by Diffused Heads [66], though unlike their approach, we use spectral features rather than features extracted from a pretrained speech encoder in order to capture as much information about the signal as possible. To the best of our knowledge, this is the first work that applies denoising diffusion models to the task of audio-driven video editing. As part of this work, we state the following contributions to the field:

- A novel unstructured end-to-end approach for audio-driven video editing using a denoising diffusion model. We condition the network on speech and train it to modify the face such that the lip and jaw movements are synchronised to the conditioning audio signal on a frame-by-frame basis. We train both single, and multi-speaker proof-of-concept models using the GRID [14], and CREMA-D [6] datasets respectively, achieving strong proof-of-concept results when tested on unseen speakers. The project code, datasets, and trained models will be made freely available to the public.

- We demonstrate the applicability of our approach on the video editing task, achieving competitive results thanks to our conditional inpainting strategy which gathers information from previous frames and audio spectral embeddings, to generate the current frame. Our method achieves near state-of-the-art results when measured on traditional image quality metrics such as SSIM, PSNR, FID, and competitive SyncNet [13] lip synchronisation scores compared to other relevant methods from the field.

2. Related Works

2.1. Audio Driven Video Generation

Audio-driven video generation methods can generally be categorised by whether they are generated by leveraging an audio-driven structural representation of the face, or without.

There have been numerous approaches over the years relating to the former. Taylor et al. [69] and Karras et al. [32] among the first to apply machine learning techniques to the facial animation task, the former learning facial expression parameters of a 3D face model from phoneme labels, and the latter predicting 3D vertex positions of a face mesh from a speech audio window. Suwajanakorn et al. [67] trained a speaker specific network to output sparse mouth key-points, using them to modify videos of President Obama. Eskimez et al [17] presented a recurrent architecture capable of taking in speech as input and outputting 2D landmark face coordinates, with Chen et al. [9] utilising cascaded GANs to translate those landmark features into photorealistic frames. Cudeiro et al. [15] introduced a 4D facial dataset, and trained a network to generate animations from speech with it. [5, 40, 73, 88] generated intermediate landmark features from audio, also exploring the related task of extracting realistic headpose. Thies et al. [70] generated 3D facial expression parameters using features from a pretrained audio encoder, using these parameters to generate a photorealistic video via a neural renderer, with [75] and [63] following a similar approach but operating on videos instead. [7] and [81] presented methods to generate 3D face animation parameters, in addition to realistic head pose from speech, using these features to generate photorealistic frames. Ji et al. [31] approached the problem of video editing, generating emotion-controllable talking head portraits using both intermediate landmark structures, and 3D model parameters. [37, 54, 62, 76, 82, 84] are other approaches from the literature which predict expression parameters from audio to drive a 3D face model.

What these approaches all have in common is that they use these intermediate structural representations as input to a separate neural rendering model which is typically trained as an image-to-image translation task to generate the final photo-realistic image frame. As of the date of this submission, GAN-based [20] approaches such as Pix2Pix [28], CycleGAN [90], and other variations have proved immensely popular for this task. However, diffusion-based techniques show big promise for the future, especially given recent developments in various image-to-image translation tasks [58].

Nonstructural/end-to-end methods on the other hand

utilise latent feature learning and image reconstruction techniques to generate a photo-realistic video sequence from an input speech signal and reference image/video in an end-to-end manner. Approaches such as [8, 18, 29, 36, 44, 50, 65, 72, 86, 87, 89] have seen much success in recent times. Each of these approaches differs from the one used in this paper as they are all GAN/VAE (variational autoencoder) [34] based probabilistic methods while ours leverages a denoising diffusion model. While current end-to-end approaches suffer from low output resolution quality compared to structural methods, there is a lot of potential for improvement, especially by exploiting diffusion models' ability to synthesise high-quality samples while maintaining good mode coverage/diversity.

2.2. Diffusion Models

Denoising diffusion models [61, 64] have seen great success on a wide variety of different challenges, ranging from image-to-image translation tasks like inpainting, colorisation, image upscaling, uncropping [4, 25, 42, 43, 51, 55, 58, 60], audio generation [10, 27, 33, 35, 38, 49, 68, 78], text-based image generation [2, 19, 21, 47, 53, 57, 59], video generation [22, 26, 80, 83], and many others. Recently, diffusion models have also been applied to the related task of talking head generation, with the work of [66] a concurrent approach to our own. For a thorough review of diffusion models and all of their recent applications, we recommend [79].

Diffusion models are a class of generative probabilistic models that consist of two steps: 1) the forward diffusion process that destroys data by steadily adding small amounts of random Gaussian noise over a series of time steps until the data becomes a sample from a standard Gaussian distribution. 2) The reverse diffusion process where a denoising model is trained to restore structure in the data by steadily removing noise over a series of time steps. The trained model can then sample information from random Gaussian noise and steadily denoise it over a series of time steps to attain the desired output.

Sohl-Dickstein et al. [61] developed the first diffusion model and coined the term, followed by Ho et al. [24] combining denoising score matching with Langevin dynamics [64] and diffusion models to synthesise images. This ignited a steady interest in diffusion models, with Nichol et al. [48] showing that by making small adjustments to the diffusion process, they could sample data faster and achieve better log-likelihoods to models trained explicitly to minimise it with minimal impact to sample quality. They also found that training diffusion models with more computational power typically lead to better sample quality. Chen et al. [10] and Kong et al. [35] applied diffusion models to the task of audio synthesis, succeeding in generating high-quality samples. Dhariwal and Nichol [16] demonstrated that diffusion models beat GANs on image synthesis, also introducing the concept of "classifier guidance" for a conditional generation.

As diffusion models are trained under a single loss and do not rely on a discriminator, they are more stable during training and do not suffer from typical issues associated with training GANs such as mode collapse, and vanishing gradients. They produce high-quality output samples and display high mode coverage unlike GANs [77]. Despite these advantages, their sampling speed is slow due to the need to run the inverse diffusion process thousands of times on the same sample to denoise it completely. Xiao et al. [77] and Rombach et al [55] attempted at speeding up the sampling and training times associated with diffusion models with the former proposing a method to model the denoising distribution using a complex multi-modal distribution in order to facilitate larger diffusion steps, and the latter applying diffusion models in the latent space of a pre-trained autoencoder to reduce the complexity. This is an ongoing focus of research in the field, and it is a certainty that more works tackling the inference/training speed problem will emerge.

3. Methodology

A diffusion model is defined as having two steps, the forward diffusion process where the data is gradually destroyed, and the learned inverse diffusion process which reconstructs the data, and is used during training and inference. In our case, we condition a denoising U-Net on image and speech features to denoise a masked portion of the target frame into the desired output. A high-level overview of this process is depicted in figure 1.

3.1. Diffusion process

3.1.1 Forward diffusion process

As defined by [61], the forward diffusion process is a Markov chain that adds small amounts of noise to the data y over a predefined number of time steps T, until the data is completely destroyed at time step t=T. This state is represented as y_T with y_0 representing the data before any noise was added to it. The Markov chain is defined by:

$$q\left(y_{1:T}|y_0\right) := \prod_{y=1}^{T} q\left(y_t|y_{t-1}\right) \tag{1}$$

where at each step, Gaussian noise is added by:

$$q\left(y_t|y_{t-1}\right) := \mathcal{N}\left(y_t; \sqrt{\alpha_t}y_{t-1}, (1-\alpha_t)I\right), \tag{2}$$

with $\alpha_t := (1-\beta_t)$, representing the hyperparameters of our fixed noise scheduler. [24] show that it is possible to sample y_t at any step t in closed form:

$$q\left(y_t|y_0\right) := \mathcal{N}\left(y_t; \sqrt{\bar{\alpha}_t}y_0, (1-\bar{\alpha}_t)I\right), \tag{3}$$

with $\bar{\alpha}_t := \prod_{s=1}^{t} \alpha_s$. This is an important observation, as it significantly speeds up the forward diffusion process, and can be used to train a model on the fly with random noise levels at each forward step.

3.1.2 Inverse diffusion process

Given a noisy image $\bar{y}$ defined as:

$$\bar{y} := \sqrt{\bar{\alpha}} y_0 + \sqrt{1-\bar{\alpha}}\epsilon, \epsilon \sim \mathcal{N}(0, I) \tag{4}$$

the goal of the Inverse diffusion process is to learn an algorithm that can denoise and restore the noisy image to its original image Y_0. Following the approach in [58], we train a neural network $f_\theta(x, \bar{y}, \bar{\alpha}, \omega)$, a 2D U-Net [56], to predict the noise generated at time t, optimising the L_{simple} objective proposed by [24]:

$$\mathbb{E}_{t, y_0, \epsilon}\left[\left\| f_\theta(x, \sqrt{\bar{\alpha}} y_0 + \sqrt{1-\bar{\alpha}}\epsilon, \bar{\alpha}, \omega) - \epsilon \right\|^2 \right] \tag{5}$$

where x represents the identity and previous frame input to our network, $\bar{y}$ the noisy image, $\bar{\alpha}$ the noise level, and ω the audio features. During training, we only calculate the loss for the masked region of the face to conserve computational resources, following the approach in [58].

Following [24], to run inference, each step of the inverse diffusion process can then be computed by:

$$y_{t-1} \leftarrow \frac{1}{\sqrt{\alpha_t}}\left(y_t - \frac{1-\alpha_t}{\sqrt{1-\bar{\alpha}_t}} f_\theta(x, y_t, \bar{\alpha}_t) \right) + \sqrt{1-\alpha_t}\epsilon_t, \tag{6}$$

where $\epsilon \sim \mathcal{N}(0, I)$. The inverse diffusion step is then repeated T times. Please see figure 1 for a high-level view of our network architecture, and to better understand where each equation is used. For a more detailed discussion behind these equations, and how they are derived, please see [24, 61, 64].

3.2. Model Architecture

Figure 1 depicts the overall architecture of our model. We frame the problem of audio-driven video editing as a conditional inpainting task with a few key changes. Traditionally, inpainting is an image-to-image translation task where a neural network must learn to fill in a masked out region of the image with realistic content. For video editing, we must provide the network with additional context, to help guide its generation process. To do this, we split the conditioning step into two categories, frame-based, and audio-based conditioning.

Frame-Based Conditioning: For a given frame y^i extracted from a video consisting of frames (y^0,...,y^n), our model takes three images as input: 1) the current *masked noisy frame* y_T^i that is to be inpainted, 2) the *previous frame* $y^{(i-1)}$ in the video sequence, and 3) a constant *identity frame* y^0. As our approach is auto-regressive and works on a frame-by-frame basis, the purpose of the previous frame is to ensure that there is temporal stability between consecutive frames. Omitting it causes the model to output jittery, unstable frames. The identity frame is there to encourage the model not to deviate away from the target identity during the generation process, as so often is the case with auto-regressive models. While the identity frame can be omitted if training a single-speaker model with little to no adverse effects, we found that its inclusion was key to having a model that could generalise well to unseen subjects when training on multiple identities. These three frames are concatenated channel-wise, and fed into the U-Net as an input feature of size [128x128x9], as depicted on the left hand side of figure 1.

Audio-Based Conditioning:

For a given video sequence of frames (y^0 ,..., y^n), there is a corresponding sequence of audio spectral features ($spec^0$,..., $spec^{2n}$) extracted from the original speech signal. Each audio feature spans a 40ms window, overlapping every 20ms. Details on how we compute these features are provided in section 3.3. In order to provide the audio information to the network, we extract a window of audio from ($spec^{2i-2}$ to $spec^{2i+2}$) spanning 120 ms denoted as z^i that is centered around the current video frame y^i. We do this so that audio information from both the preceding and following frames is captured within the window to guarantee the accurate production of lip movements for plosive sounds ("p, t, k, b, d, g") by taking into consideration that these lip movements precede the sound production. We introduce this information to the U-net via the use of conditional residual blocks that condition the network on audio and noise level embeddings, scaling and shifting the hidden states of the U-net following the approach of [66]:

$$h_{s+1} = z_s^i(t_s GN(h_s + t_b)) + z_b^i \tag{7}$$

where h_s and h_{s+1} represent consecutive hidden states of the U-Net, (z_s^i, z_b^i) = MLP(z^i), and (t_s, t_b) = MLP($\bar{\alpha}_t$). MLP represents a shallow neural network with a couple of linear layers separated by a SiLu() activation function, and GN is a group normalisation layer. This is shown in figure 1.

U-Net Set Up: In order to denoise the current noisy frame, we use a denoising U-net [56], following the general architecture described by [58], which in turn is based on the model proposed by [24] with modifications inspired by the works of [16, 60]. For this work we use a lightweight 128x128 version of the 256x256 U-net architecture described by [16], omitting the class conditioning mechanism. Like [58] we condition the model to generate the desired frames via the concatenation of the previous and identity frames to the masked frame. We drive the facial animation by sending audio features throughout conditional residual

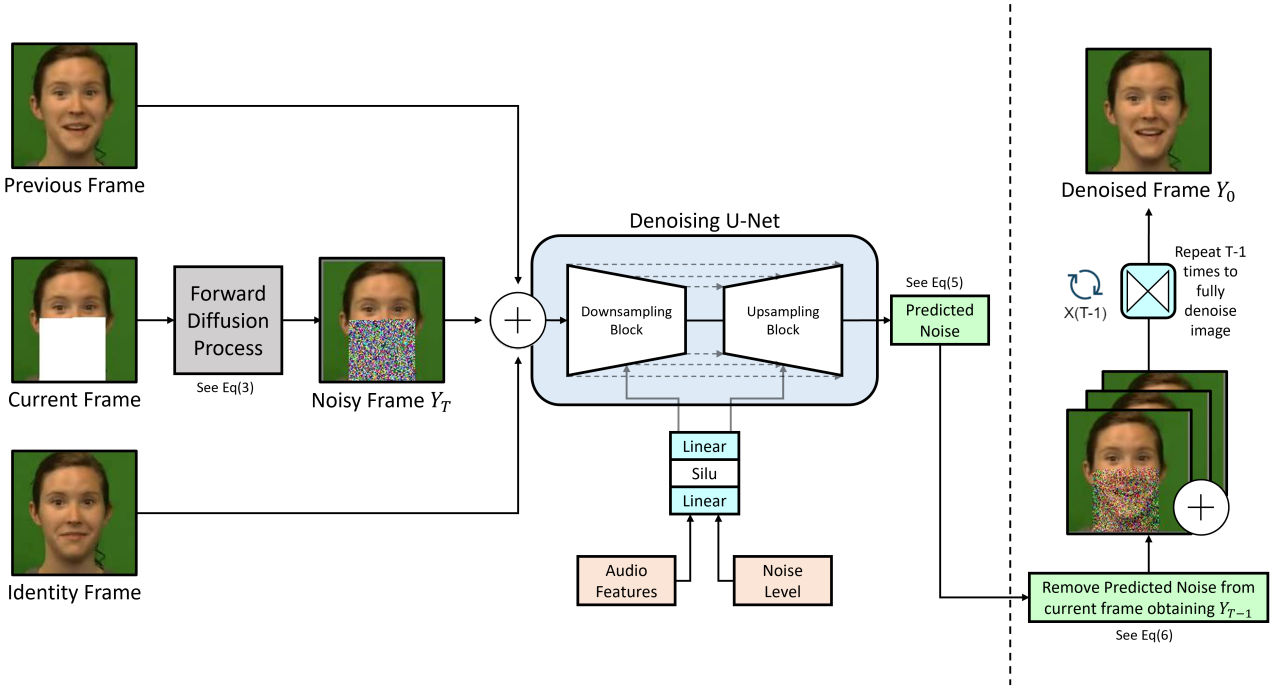

Figure 1. High-level overview of the network architecture. Left of the dashed line indicates the training procedure, right of it depicts the inference procedure. $\bigoplus$ represents the concatenation operator, and $\dashrightarrow$ represents a skip connection. The current frame is passed through the forward diffusion process where the noise is computed and added to the masked region of the face, obtaining noisy frame Y_t (Equation 3). The previous and identity frames are then concatenated channel-wise to it, forming a 128x128x9 feature and passed to the U-net directly. Audio features and noise level information are fed into the U-net through conditional residual blocks as described in equation 7. During inference, the predicted noise is removed from noisy image Y_t, obtaining Y_{t-1}. The previous and identity frames are concatenated to Y_{t-1}, and the process is repeated until the image is fully denoised (Equation 6).

blocks within the U-Net as detailed by [66], described by equation 7. We include all details related to our U-Net configuration in table 1.

Table 1 displays the hyperparameters we use to train our diffusion model for the task of audio-driven video editing. We train two models, a single-speaker model trained on identity S1 of the GRID dataset, and a multispeaker model trained on the train set of the CREMA-D dataset. A notable difference between the two models is the use of attention. For the single-speaker model, we omitted it from the up/downsampling layers of the U-Net, using it only within the middle block in an effort to boost training speed. Despite this, we still obtain pleasing results, as shown both in table 2, and in the videos provided as part of the supplementary materials. During our experiments, we discovered that the use of attention within the multi-speaker model was crucial for it to generalise well to both seen and unseen speakers. We apply it at resolutions of 32x32 within the up/downsampling layers of the U-Net. We provide more discussion on this in section 4. To perform training we used a server of 4 32GB V100 GPUs, allowing us a batch size of 40 per GPU.

	Single ID	Multi-ID
Image Size	$128x128$	$128x128$
Total Frames	73704	432000
Diffusion Steps	2000	1000
Noise Schedule	$Linear$	$Cosine$
Linear Start	$1e-06$	NA
Linear End	0.01	NA
Input Channels	10	10
Inner Channels	64	64
Channels Multiple	$1, 2, 4, 8$	$1, 2, 3$
Attention Resolution	NA	32
Res Blocks	2	2
Head Channels	32	32
Drop Out	0.2	0.2
Batch Size	10	40
Training Epochs	2000	735
Learning Rate	$5e-05$	$5e-05$

Table 1. U-Net Training Hyperparameters

3.3. Data Processing

3.3.1 Dataset

We rely on the GRID [14], and CREMA-D [6] audio-visual speech data sets to carry out the work in this paper. GRID is a multi-speaker data set consisting of 34 speakers (18 male, 16 female), with each speaker uttering 1000 short 6-word sentences. CREMA-D is a multi-speaker dataset consisting of 7,442 talking head clips of 91 speakers from diverse ethnic backgrounds. We present two models: 1) A single speaker model trained on 950 videos from the speaker 1 of the GRID dataset, with the model's performance being evaluated on the remaining 50 videos on the task of video editing. 2) A multi-speaker model trained on a majority of the CREMA-D dataset, with videos from identities 15, 20, 21, 30, 33, 52, 62, 81, 82, and 89 kept hidden from the model for testing and evaluation purposes.

3.3.2 Audio Preprocessing

From each video within the GRID and CREMA-D datasets, we extract the audio files and resample them at 16Khz. From the audio we compute overlapping mel-spectrogram features with n-fft 2048, window length 640, hop length 320, and 256 mel bands. With these values, a 1-second audio feature has a shape [50,256] that can be easily aligned to a sequence of video frames.

3.3.3 Video Preprocessing

First, we perform a 128x128 pixel crop centered around the face on every video frame. We do this by aligning the face in the video to the canonical face with a smoothing window of 7 frames, following the approach of [71]. We do this for two reasons: To get rid of any irrelevant background, and to reduce the image size to facilitate faster training and convergence speeds. In our initial experiments, we used an image size of 256x256 however the model was too expensive to train on our limited resources. It is worth noting that a video super-resolution technique such as [39] may be applied on top of our solution to achieve high-resolution samples.

Next, every video frame needs to have a rectangular region of the face masked out. Using an off-the-shelf facial landmark extractor [41], we extract facial landmark coordinates to determine the position of the jaw. Using this information, we mask out a rectangular portion of the face that covers a region just below the nose, as within figure 1. This face mask is computed and applied to the frames at train time within the data loader on the fly.

During training, it is critical to hide the speaker's jawline with a rectangular face mask. This is because the network can easily pick up on the strong correlation between lip and jaw movements, leading it to ignore the speech input entirely. By hiding the jawline, we compel the model to learn to generate lip movements based solely on the accompanying speech. As the diffusion process relies on a single loss function, applying the rectangular face-mask is the easiest way to prevent the frame-based input dominating over the speech input.

3.3.4 Audio Video Alignment:

As described previously in section 3.2, given a video sequence with frames (y^0 ,..., y^n), there is a corresponding sequence of audio spectral features ($spec^0$,..., $spec^{2n}$) extracted from the original speech signal. Each audio feature spans a 40ms window, overlapping every 20ms. For any given frame Y^i, it is aligned to audio features spanned by ($spec^{2i-2}$ to $spec^{2i+2}$). To align the first and last video frames, we simply append silence to the start, and ends of their respective audio features. Care must be taken when choosing the audio window, too large and the network won't use the most meaningful information available to it, too small and there may not be enough context for the network to generate more complex lip movements caused by plosives.

4. Experiments & Results

In this section we present two models. A single-speaker video editing model trained on speaker S1 from the GRID dataset, and a multi-speaker model trained on the train-split of the CREMA-D dataset. We evaluate and compare our results to other recent audio-driven video generation methods, namely EAMM [30], PC-AVS [87], MakeItTalk [88], Speech Driven Animation [72], and Wav2Lip [50]. All models we test against are relevant end-to-end image-reconstruction based methods, except for MakeItTalk, a landmark-based method we compare against for reference purposes. We evaluate these models on the CREMA-D multispeaker test set, reporting their scores along with our own in table 2. We generate the videos for each model using the official publicly available implementations with the recommended parameters.

As our models are trained explicitly for video editing, they generate only a small portion of the overall frame, while keeping the rest as is. Therefore, to maintain fairness, all metrics that rely on comparing the generated frame to the ground truth are computed only on the generated portion of the image. This limitation could also create bias in the perceptual metrics and readers should consider this when comparing our model scores to others within the literature.

We emphasise that the objective of this paper is to serve as a proof-of-concept demonstrating the potential of applying denoising diffusion models to the task of audio-driven video editing. As such, while we do not achieve state-of-the-art in some of the metrics we report, our results still

Method	LSE-C↑	LSE-D↓	FID	SSIM↑	PSNR↑	CPBD
Ground Truth CREMA-D	5.45	8.12	-	-	-	-
EAMM (Actual)	3.98	8.92	22.52	0.74	29.43	0.1
EAMM (Random)	3.95	8.98	23.04	0.72	29.21	0.124
PC-AVS (Actual)	6.12	7.8	38.46	0.61	28.47	0.127
PC-AVS (Randon)	6.07	7.82	40.05	0.59	28.42	0.11
SpeechDrivenAnimation	-	-	155.63	0.844^{*}	27.98^{*}	0.277^{*}
Wav2Lip(Actual)	5.89	7.57	16.21	0.886	34.23	0.253
Wav2Lip(random)	5.6	7.89	20.23	0.872	34.04	0.247
Make It Talk	3.5	9.71	27.35	0.75	31.37	0.152
Ours (MultiSpeaker - 100)	3.53	9.74	$2.362^{\dagger}$	0.893	34.32	0.26
Ours (MultiSpeaker - 500)	3.5	9.68	$2.13^{\dagger}$	0.902	34.4	0.26
Ours (MultiSpeaker - 1000)	3.49	9.69	$2.369^{\dagger}$	0.863	34.12	0.242
Ours (Single Speaker)	4.98	7.59	$2.312^{\dagger}$	0.92	32.47	0.29

Table 2. Quantitative comparison with previous works on image quality and lip synchronization metrics. Most previous works we compare to require a driving video to guide the pose of the generated speaker. For these approaches (Actual) indicates whether we provided the ground truth video to their model in addition to the ground truth audio to generate the new video, while (Random) indicates that we used a random audio file instead. We report their results under both configurations to maintain fairness. For our models we also indicate how many diffusion timesteps were used to generate the frames during inference. We report results for 100, 500, and 1000 inference steps. † indicates that this metric was computed on the full frame. * indicates that these results are reported from their paper.

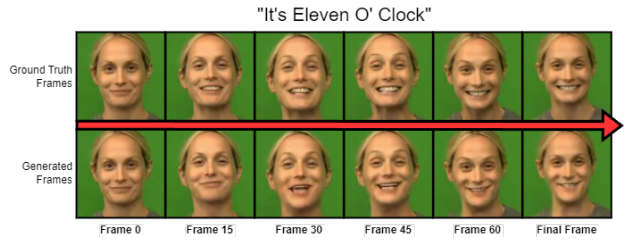

Figure 2. Multi-speaker failure case: Over time the appearance of the speaker slowly drifts away from the original.

show promising improvements over existing methods and highlight the potential of using denoising diffusion models for this task instead of traditional GAN-based methods.

4.1. Evaluation Metrics

We use a number of objective metrics to measure the quality of our generated videos, allowing us to compare them directly to other state-of-the-art audio-driven video generation methods from the literature. We compute SSIM [74] (Structural Similarity Index Measure) ↑, PSNR (Peak Signal to Noise Ratio) ↑, and FID [23] (Frechet Inception Distance) ↓ scores for the generated videos against their corresponding ground truth to measure the overall quality of the generated frames. We also compute CPBD [46] (Cumulative Probability Blur Detection) ↑ scores, and SyncNet [13, 50] Confidence (LSE-C) ↑ and Distance (LSE-D) ↓ scores. We reiterate the point that in order to maintain fairness when computing the image quality metrics, we only compute them on the generated portion of the image where possible.

4.2. Single Speaker

We train our single speaker model on identity S1 using data from the GRID audio-visual corpus [14]. There are 1000 videos in total, each of them roughly 3 seconds in length totaling about 50 minutes of audio-visual content for training. We train our model on 950 videos, withholding 50 of them for testing purposes. We train this model for 895 Epochs. As we mentioned previously, we did not use any attention layers within the up/downsampling blocks of this model, using it just within the middle block of the U-Net. We did this to save on training time, however, for stronger results we recommend using it, as we show within our multi-speaker model.

4.3. Multi-Speaker

We train our multi-speaker model on all identities of the CREMA-D data set except for speakers 5, 20, 21, 30, 33, 52, 62, 81, 82, and 89, choosing to keep them hidden from the model for testing purposes. We train the model for 735 Epochs. There are a number of key changes we make to train the multi-speaker model. First, we use self-attention layers within the U-Net at the 32x32 resolution, as well as in the middle block. Second, we switch to a cosine noise schedule and decrease the number of diffusion steps taken by the model during training to 1000. Finally, we decrease the number of channel multiples to [1,2,3]. We also experimented with training a model without attention in the up/downsampling blocks. It failed to converge on even train set identities. We speculate that increasing the number of inner channels used by our U-Net from 64 to 128 or 256 would significantly improve the results, as well as training

the model for a longer amount of time. Please see table 2 for a summary of our experiments and evaluations, compared to other popular works in the literature, and section 4.4 for a detailed discussion surrounding the results.

4.4. Results Discussion

Table 2 depicts the results our models score when tested on their unseen test sets versus other approaches in the literature. While the results we obtain are not state-of-the-art in all metrics, they successfully demonstrate that using a denoising diffusion model to do audio-driven video editing, is indeed quite feasible, and produces high-quality results comparable to other relevant methods in the literature.

The multi-speaker model generalises quite well to unseen speakers, scoring highly on image quality metrics, managing to outperform all other methods except for Wav2Lip on SSIM and CPBD. The single speaker model also achieving similarly strong results. We believe that this is due to the diffusion models inherent ability to model complex, high-dimensional data distributions, allowing it to learn the statistical properties of the dataset and generate images that are similar to those in the training set. Further, as diffusion models are trained to gradually remove noise from the target image over time, this may help it generate smoother, and more visually pleasing results than those generated by a GAN-based model which generates the frame in one shot. Within the context of audio-driven video editing, achieving visually pleasing results is a key requirement that our model fulfills. Please see the videos attached in the supplementary material for a visual comparison between our method and existing ones.

When evaluated on SyncNet [13] confidence (LSE-C) and distance (LSE-D) scores, our multi-speaker results are comparable to other popular methods from the literature, slightly outperforming MakeItTalk, but scoring lower than EAMM. PC-AVS and Wav2Lip score the highest in that order. Notably, their approaches significantly outperform the ground truth. We believe that this is because all other methods are specifically trained to optimise a loss function designed to penalise their models for poor lip synchronisation. In the case of PC-AVS and Wav2Lip, they both rely on a strong lip sync discriminator, to encourage their models to generate distinct, clear lip movements given speech. Our approach uses no such losses or discriminators, inherently learning the relationship between speech and lip movement during training. As such while our lip synchronisation scores on unseen speakers are lower, we offer a novel approach to the task as we do not explicitly train the model to improve lip synchronisation.

It is also worth noting that our single-speaker model performs very well on the synchronisation metrics mentioned above, leading us to speculate that with more time spent learning the data distribution, our multi-speaker model could also theoretically achieve such results.

During inference, we noticed that the multi-speaker model occasionally struggled to maintain the identity consistent throughout the generation process, with the problem especially prevalent if there were extreme changes in head pose present in the original video. This is due to a buildup of small errors, as our approach is completely auto-regressive at inference time, relying entirely on just the previously generated frame, and identity frame to modify the current frame. Figure 2 highlights one such instance of failure, and the phenomenon is noticeable in some of the videos we provide in our video abstract. We speculate that this could be alleviated in three ways 1) introducing small amounts of face warping on the previous frame during training in order to simulate the distortion that naturally occurs over the generation process. This would encourage the model to look at the identity frame in order to correct itself. 2) Simply train the model for longer. 3) Train on a more diverse dataset of speakers captured in unconstrained conditions such as VoxCeleb or LRS.

When testing on identities seen by the network during training by replacing the original audio with a new one, the model achieves strong lip synchronisation, and the identity deviation seen when testing on unseen identities is significantly diminished, or simply does not occur over the course of the video. This problem is also non-existent in our single-speaker model.

We also observed that the multi-speaker model is highly sensitive to speaker volume, and intonation, especially when exposed to speech from unseen speakers. In instances where the speaker shouts or speaks loudly and clearly at the microphone, the lip movement is highly accurate and appears well-synchronised. When the volume is low, the speaker appears to be mumbling, and the full range of lip motion is not correctly generated. Analysing the synchronisation metrics confirmed this for us, with videos generated using audio labelled as being "angry" or "happy", scoring significantly higher than instances where the portrayed emotion was "sad", "fearful", or "disappointed". We suspect that this is due to our use of spectral feature embeddings when conditioning our network, and could be alleviated or significantly diminished with the use of a pre-trained audio encoder for speech recognition. This is because such models are typically trained to extract the content from speech, disregarding information considered irrelevant such as pitch, or tone, and intonation.

5. Future Work

Model Speed and In The Wild Training: It is no secret that diffusion models are slow, both to train and to sample from. Our models are no exception, taking us approximately 6 minutes/epoch to train the single-speaker model, and 40 minutes/epoch for the multi-speaker one. We briefly

experimented with training in the latent space to speed up training following the approach of [55], however, sample quality suffered, so we decided to operate in the pixel space. We intend to revisit this however as improving our models training speed is a top priority for us as it would allow us to train on larger, more diverse, "in-the-wild" datasets such as VoxCeleb [45], or LRS [12].

Appearance Consistency: As previously discussed, our multi-speaker model's generated output appearance for unseen identities occasionally deviates from the original. To investigate this phenomenon, we intend to delve deeper into the underlying causes. Specifically, we will explore whether this effect is due to inadequate training or insufficient diversity in the training dataset, or a combination of both. By conducting a more detailed analysis, we hope to gain a better understanding of how to optimize our model's performance for a wider range of identities. Further, we intend to fully train a model that utilises the face warping augmentation to determine whether this truly provides a positive impact on the generated samples.

Speech Conditioning: We plan to explore the potential of conditioning our model with a wider range of speech features, such as experimenting with larger or smaller window sizes when computing spectral features or using pre-trained audio encoders such as Wav2Vec2 [3], Whisper [52], or DeepSpeech2 [1]. We believe that incorporating such features could potentially improve the lip synchronization performance of our model and generate even more realistic and expressive lip movements.

6. Conclusion

Our results showcase the versatility of denoising diffusion models in capturing complex relationships between audio and video signals and generating coherent video sequences with accurate lip movements for the task of speech-driven video editing. We are encouraged by the strong performance achieved by our proof-of-concept approach, scoring highly on all tested metrics, comparable to existing state of the art in end-to-end video generation.

However, our work is not without limitations. The CREMA-D dataset is relatively small compared to other publicly available speech and video datasets, which limits the generalizability of our approach to other domains. Additionally, our approach requires a significant amount of computational resources and time to train. This is a challenge for real-time applications or for training on large-scale datasets.

We are confident that our work will inspire further research and development in this area, leading to more efficient and effective methods for speech-driven video editing. With the continuing advancements in machine learning and computer vision, we believe that denoising diffusion models will play an increasingly important role in enabling high-quality and immersive multimedia experiences that can better reflect the diversity and richness of human communication.

References

[1] Dario Amodei, Sundaram Ananthanarayanan, Rishita Anubhai, Jingliang Bai, Eric Battenberg, Carl Case, Jared Casper, Bryan Catanzaro, Qiang Cheng, Guoliang Chen, et al. Deep speech 2: End-to-end speech recognition in english and mandarin. In *International conference on machine learning*, pages 173–182. PMLR, 2016. 9

[2] Omri Avrahami, Dani Lischinski, and Ohad Fried. Blended diffusion for text-driven editing of natural images. In *Proceedings of the IEEE/CVF Conference on Computer Vision and Pattern Recognition*, pages 18208–18218, 2022. 3

[3] Alexei Baevski, Yuhao Zhou, Abdelrahman Mohamed, and Michael Auli. wav2vec 2.0: A framework for self-supervised learning of speech representations. *Advances in neural information processing systems*, 33:12449–12460, 2020. 9

[4] Georgios Batzolis, Jan Stanczuk, Carola-Bibiane Schönlieb, and Christian Etmann. Conditional image generation with score-based diffusion models. *arXiv preprint arXiv:2111.13606*, 2021. 3

[5] Sandika Biswas, Sanjana Sinha, Dipanjan Das, and Brojeshwar Bhowmick. Realistic talking face animation with speech-induced head motion. In *Proceedings of the Twelfth Indian Conference on Computer Vision, Graphics and Image Processing*, pages 1–9, 2021. 2

[6] Houwei Cao, David G. Cooper, Michael K. Keutmann, Ruben C. Gur, Ani Nenkova, and Ragini Verma. Crema-d: Crowd-sourced emotional multimodal actors dataset. *IEEE Transactions on Affective Computing*, 5(4):377–390, 2014. 2, 6

[7] Lele Chen, Guofeng Cui, Celong Liu, Zhong Li, Ziyi Kou, Yi Xu, and Chenliang Xu. Talking-head generation with rhythmic head motion. In *European Conference on Computer Vision*, pages 35–51. Springer, 2020. 1, 2

[8] Lele Chen, Zhiheng Li, Ross K Maddox, Zhiyao Duan, and Chenliang Xu. Lip movements generation at a glance. In *Proceedings of the European Conference on Computer Vision (ECCV)*, pages 520–535, 2018. 2, 3

[9] Lele Chen, Ross K Maddox, Zhiyao Duan, and Chenliang Xu. Hierarchical cross-modal talking face generation with dynamic pixel-wise loss. In *Proceedings of the IEEE/CVF conference on computer vision and pattern recognition*, pages 7832–7841, 2019. 2

[10] Nanxin Chen, Yu Zhang, Heiga Zen, Ron J Weiss, Mohammad Norouzi, and William Chan. Wavegrad: Estimating gradients for waveform generation. *arXiv preprint arXiv:2009.00713*, 2020. 3

[11] Sen Chen, Zhilei Liu, Jiaxing Liu, and Longbiao Wang. Talking head generation driven by speech-related facial action units and audio-based on multimodal representation fusion. *arXiv preprint arXiv:2204.12756*, 2022. 2

[12] Joon Son Chung, Andrew Senior, Oriol Vinyals, and Andrew Zisserman. Lip reading sentences in the wild. In *2017*

IEEE conference on computer vision and pattern recognition (CVPR), pages 3444–3453. IEEE, 2017. 9

[13] J. S. Chung and A. Zisserman. Out of time: automated lip sync in the wild. In *Workshop on Multi-view Lip-reading, ACCV*, 2016. 2, 7, 8

[14] Martin Cooke, Jon Barker, Stuart Cunningham, and Xu Shao. An audio-visual corpus for speech perception and automatic speech recognition. *The Journal of the Acoustical Society of America*, 120(5):2421–2424, 2006. 2, 6, 7

[15] Daniel Cudeiro, Timo Bolkart, Cassidy Laidlaw, Anurag Ranjan, and Michael J Black. Capture, learning, and synthesis of 3d speaking styles. In *Proceedings of the IEEE/CVF Conference on Computer Vision and Pattern Recognition*, pages 10101–10111, 2019. 2

[16] Prafulla Dhariwal and Alexander Nichol. Diffusion models beat gans on image synthesis. *Advances in Neural Information Processing Systems*, 34:8780–8794, 2021. 2, 3, 4

[17] Sefik Emre Eskimez, Ross K Maddox, Chenliang Xu, and Zhiyao Duan. Generating talking face landmarks from speech. In *International Conference on Latent Variable Analysis and Signal Separation*, pages 372–381. Springer, 2018. 2

[18] Sefik Emre Eskimez, Ross K Maddox, Chenliang Xu, and Zhiyao Duan. End-to-end generation of talking faces from noisy speech. In *ICASSP 2020-2020 IEEE International Conference on Acoustics, Speech and Signal Processing (ICASSP)*, pages 1948–1952. IEEE, 2020. 1, 3

[19] Wan-Cyuan Fan, Yen-Chun Chen, DongDong Chen, Yu Cheng, Lu Yuan, and Yu-Chiang Frank Wang. Frido: Feature pyramid diffusion for complex scene image synthesis. *arXiv preprint arXiv:2208.13753*, 2022. 3

[20] Ian Goodfellow, Jean Pouget-Abadie, Mehdi Mirza, Bing Xu, David Warde-Farley, Sherjil Ozair, Aaron Courville, and Yoshua Bengio. Generative adversarial networks. *Communications of the ACM*, 63(11):139–144, 2020. 2

[21] Shuyang Gu, Dong Chen, Jianmin Bao, Fang Wen, Bo Zhang, Dongdong Chen, Lu Yuan, and Baining Guo. Vector quantized diffusion model for text-to-image synthesis. In *Proceedings of the IEEE/CVF Conference on Computer Vision and Pattern Recognition*, pages 10696–10706, 2022. 3

[22] William Harvey, Saeid Naderiparizi, Vaden Masrani, Christian Weilbach, and Frank Wood. Flexible diffusion modeling of long videos. *arXiv preprint arXiv:2205.11495*, 2022. 3

[23] Martin Heusel, Hubert Ramsauer, Thomas Unterthiner, Bernhard Nessler, and Sepp Hochreiter. Gans trained by a two time-scale update rule converge to a local nash equilibrium. *Advances in neural information processing systems*, 30, 2017. 7

[24] Jonathan Ho, Ajay Jain, and Pieter Abbeel. Denoising diffusion probabilistic models. *Advances in Neural Information Processing Systems*, 33:6840–6851, 2020. 2, 3, 4

[25] Jonathan Ho, Chitwan Saharia, William Chan, David J Fleet, Mohammad Norouzi, and Tim Salimans. Cascaded diffusion models for high fidelity image generation. *J. Mach. Learn. Res.*, 23:47–1, 2022. 3

[26] Jonathan Ho, Tim Salimans, Alexey Gritsenko, William Chan, Mohammad Norouzi, and David J Fleet. Video diffusion models. *arXiv preprint arXiv:2204.03458*, 2022. 3

[27] Rongjie Huang, Zhou Zhao, Huadai Liu, Jinglin Liu, Chenye Cui, and Yi Ren. Prodiff: Progressive fast diffusion model for high-quality text-to-speech. In *Proceedings of the 30th ACM International Conference on Multimedia*, pages 2595–2605, 2022. 3

[28] Phillip Isola, Jun-Yan Zhu, Tinghui Zhou, and Alexei A Efros. Image-to-image translation with conditional adversarial networks. In *Proceedings of the IEEE conference on computer vision and pattern recognition*, pages 1125–1134, 2017. 2

[29] Amir Jamaludin, Joon Son Chung, and Andrew Zisserman. You said that?: Synthesising talking faces from audio. *International Journal of Computer Vision*, 127(11):1767–1779, 2019. 1, 3

[30] Xinya Ji, Hang Zhou, Kaisiyuan Wang, Qianyi Wu, Wayne Wu, Feng Xu, and Xun Cao. Eamm: One-shot emotional talking face via audio-based emotion-aware motion model. In *ACM SIGGRAPH 2022 Conference Proceedings*, pages 1–10, 2022. 6

[31] Xinya Ji, Hang Zhou, Kaisiyuan Wang, Wayne Wu, Chen Change Loy, Xun Cao, and Feng Xu. Audio-driven emotional video portraits. In *Proceedings of the IEEE/CVF conference on computer vision and pattern recognition*, pages 14080–14089, 2021. 1, 2

[32] Tero Karras, Timo Aila, Samuli Laine, Antti Herva, and Jaakko Lehtinen. Audio-driven facial animation by joint end-to-end learning of pose and emotion. *ACM Transactions on Graphics (TOG)*, 36(4):1–12, 2017. 2

[33] Sungwon Kim, Heeseung Kim, and Sungroh Yoon. Guided-tts 2: A diffusion model for high-quality adaptive text-to-speech with untranscribed data. *arXiv preprint arXiv:2205.15370*, 2022. 3

[34] Diederik P Kingma and Max Welling. Auto-encoding variational bayes. *arXiv preprint arXiv:1312.6114*, 2013. 3

[35] Zhifeng Kong, Wei Ping, Jiaji Huang, Kexin Zhao, and Bryan Catanzaro. Diffwave: A versatile diffusion model for audio synthesis. *arXiv preprint arXiv:2009.09761*, 2020. 3

[36] Neeraj Kumar, Srishti Goel, Ankur Narang, and Mujtaba Hasan. Robust one shot audio to video generation. In *Proceedings of the IEEE/CVF Conference on Computer Vision and Pattern Recognition Workshops*, pages 770–771, 2020. 3

[37] Avisek Lahiri, Vivek Kwatra, Christian Frueh, John Lewis, and Chris Bregler. Lipsync3d: Data-efficient learning of personalized 3d talking faces from video using pose and lighting normalization. In *Proceedings of the IEEE/CVF conference on computer vision and pattern recognition*, pages 2755–2764, 2021. 2

[38] Alon Levkovitch, Eliya Nachmani, and Lior Wolf. Zero-shot voice conditioning for denoising diffusion tts models. *arXiv preprint arXiv:2206.02246*, 2022. 3

[39] Chengxu Liu, Huan Yang, Jianlong Fu, and Xueming Qian. Learning trajectory-aware transformer for video super-resolution. In *Proceedings of the IEEE/CVF Conference on Computer Vision and Pattern Recognition*, pages 5687–5696, 2022. 6

[40] Yuanxun Lu, Jinxiang Chai, and Xun Cao. Live speech portraits: real-time photorealistic talking-head animation. *ACM Transactions on Graphics (TOG)*, 40(6):1–17, 2021. 2

[41] Camillo Lugaresi, Jiuqiang Tang, Hadon Nash, Chris McClanahan, Esha Uboweja, Michael Hays, Fan Zhang, Chuo-Ling Chang, Ming Guang Yong, Juhyun Lee, et al. Mediapipe: A framework for building perception pipelines. *arXiv preprint arXiv:1906.08172*, 2019. 6

[42] Andreas Lugmayr, Martin Danelljan, Andres Romero, Fisher Yu, Radu Timofte, and Luc Van Gool. Repaint: Inpainting using denoising diffusion probabilistic models. In *Proceedings of the IEEE/CVF Conference on Computer Vision and Pattern Recognition*, pages 11461–11471, 2022. 3

[43] Chenlin Meng, Yang Song, Jiaming Song, Jiajun Wu, Jun-Yan Zhu, and Stefano Ermon. Sdedit: Image synthesis and editing with stochastic differential equations. *arXiv preprint arXiv:2108.01073*, 2021. 3

[44] Gaurav Mittal and Baoyuan Wang. Animating face using disentangled audio representations. In *Proceedings of the IEEE/CVF Winter Conference on Applications of Computer Vision*, pages 3290–3298, 2020. 3

[45] Arsha Nagrani, Joon Son Chung, and Andrew Zisserman. Voxceleb: a large-scale speaker identification dataset. *arXiv preprint arXiv:1706.08612*, 2017. 9

[46] Niranjan D Narvekar and Lina J Karam. A no-reference image blur metric based on the cumulative probability of blur detection (cpbd). *IEEE Transactions on Image Processing*, 20(9):2678–2683, 2011. 7

[47] Alex Nichol, Prafulla Dhariwal, Aditya Ramesh, Pranav Shyam, Pamela Mishkin, Bob McGrew, Ilya Sutskever, and Mark Chen. Glide: Towards photorealistic image generation and editing with text-guided diffusion models. *arXiv preprint arXiv:2112.10741*, 2021. 3

[48] Alexander Quinn Nichol and Prafulla Dhariwal. Improved denoising diffusion probabilistic models. In *International Conference on Machine Learning*, pages 8162–8171. PMLR, 2021. 2, 3

[49] Vadim Popov, Ivan Vovk, Vladimir Gogoryan, Tasnima Sadekova, and Mikhail Kudinov. Grad-tts: A diffusion probabilistic model for text-to-speech. In *International Conference on Machine Learning*, pages 8599–8608. PMLR, 2021. 3

[50] KR Prajwal, Rudrabha Mukhopadhyay, Vinay P Namboodiri, and CV Jawahar. A lip sync expert is all you need for speech to lip generation in the wild. In *Proceedings of the 28th ACM International Conference on Multimedia*, pages 484–492, 2020. 3, 6, 7

[51] Konpat Preechakul, Nattanat Chatthee, Suttisak Wizadwongsa, and Supasorn Suwajanakorn. Diffusion autoencoders: Toward a meaningful and decodable representation. In *Proceedings of the IEEE/CVF Conference on Computer Vision and Pattern Recognition*, pages 10619–10629, 2022. 3

[52] Alec Radford, Jong Wook Kim, Tao Xu, Greg Brockman, Christine McLeavey, and Ilya Sutskever. Robust speech recognition via large-scale weak supervision. *arXiv preprint arXiv:2212.04356*, 2022. 9

[53] Aditya Ramesh, Prafulla Dhariwal, Alex Nichol, Casey Chu, and Mark Chen. Hierarchical text-conditional image generation with clip latents. *arXiv preprint arXiv:2204.06125*, 2022. 3

[54] Alexander Richard, Michael Zollhöfer, Yandong Wen, Fernando De la Torre, and Yaser Sheikh. Meshtalk: 3d face animation from speech using cross-modality disentanglement. In *Proceedings of the IEEE/CVF International Conference on Computer Vision*, pages 1173–1182, 2021. 2

[55] Robin Rombach, Andreas Blattmann, Dominik Lorenz, Patrick Esser, and Björn Ommer. High-resolution image synthesis with latent diffusion models. In *Proceedings of the IEEE/CVF Conference on Computer Vision and Pattern Recognition*, pages 10684–10695, 2022. 2, 3, 9

[56] Olaf Ronneberger, Philipp Fischer, and Thomas Brox. U-net: Convolutional networks for biomedical image segmentation. In *International Conference on Medical image computing and computer-assisted intervention*, pages 234–241. Springer, 2015. 4

[57] Nataniel Ruiz, Yuanzhen Li, Varun Jampani, Yael Pritch, Michael Rubinstein, and Kfir Aberman. Dreambooth: Fine tuning text-to-image diffusion models for subject-driven generation. *arXiv preprint arXiv:2208.12242*, 2022. 3

[58] Chitwan Saharia, William Chan, Huiwen Chang, Chris Lee, Jonathan Ho, Tim Salimans, David Fleet, and Mohammad Norouzi. Palette: Image-to-image diffusion models. In *ACM SIGGRAPH 2022 Conference Proceedings*, pages 1–10, 2022. 2, 3, 4

[59] Chitwan Saharia, William Chan, Saurabh Saxena, Lala Li, Jay Whang, Emily Denton, Seyed Kamyar Seyed Ghasemipour, Burcu Karagol Ayan, S Sara Mahdavi, Rapha Gontijo Lopes, et al. Photorealistic text-to-image diffusion models with deep language understanding. *arXiv preprint arXiv:2205.11487*, 2022. 3

[60] Chitwan Saharia, Jonathan Ho, William Chan, Tim Salimans, David J Fleet, and Mohammad Norouzi. Image super-resolution via iterative refinement. *IEEE Transactions on Pattern Analysis and Machine Intelligence*, 2022. 3, 4

[61] Jascha Sohl-Dickstein, Eric Weiss, Niru Maheswaranathan, and Surya Ganguli. Deep unsupervised learning using nonequilibrium thermodynamics. In *International Conference on Machine Learning*, pages 2256–2265. PMLR, 2015. 2, 3, 4

[62] Luchuan Song, Bin Liu, Guojun Yin, Xiaoyi Dong, Yufei Zhang, and Jia-Xuan Bai. Tacr-net: Editing on deep video and voice portraits. In *Proceedings of the 29th ACM International Conference on Multimedia*, pages 478–486, 2021. 2

[63] Linsen Song, Wayne Wu, Chen Qian, Ran He, and Chen Change Loy. Everybody's talkin': Let me talk as you want. *IEEE Transactions on Information Forensics and Security*, 17:585–598, 2022. 2

[64] Yang Song and Stefano Ermon. Generative modeling by estimating gradients of the data distribution. *Advances in Neural Information Processing Systems*, 32, 2019. 3, 4

[65] Yang Song, Jingwen Zhu, Dawei Li, Andy Wang, and Hairong Qi. Talking face generation by conditional recurrent

adversarial network. In *Proceedings of the 28th International Joint Conference on Artificial Intelligence*, pages 919–925, 2019. 3

[66] Michał Stypułkowski, Konstantinos Vougioukas, Sen He, Maciej Zięba, Stavros Petridis, and Maja Pantic. Diffused heads: Diffusion models beat gans on talking-face generation. *arXiv preprint arXiv:2301.03396*, 2023. 2, 3, 4, 5

[67] Supasorn Suwajanakorn, Steven M Seitz, and Ira Kemelmacher-Shlizerman. Synthesizing obama: learning lip sync from audio. *ACM Transactions on Graphics (ToG)*, 36(4):1–13, 2017. 2

[68] Jaesung Tae, Hyeongju Kim, and Taesu Kim. Editts: Score-based editing for controllable text-to-speech. *arXiv preprint arXiv:2110.02584*, 2021. 3

[69] Sarah Taylor, Taehwan Kim, Yisong Yue, Moshe Mahler, James Krahe, Anastasio Garcia Rodriguez, Jessica Hodgins, and Iain Matthews. A deep learning approach for generalized speech animation. *ACM Transactions on Graphics (TOG)*, 36(4):1–11, 2017. 2

[70] Justus Thies, Mohamed Elgharib, Ayush Tewari, Christian Theobalt, and Matthias Nießner. Neural voice puppetry: Audio-driven facial reenactment. In *European conference on computer vision*, pages 716–731. Springer, 2020. 1, 2

[71] Konstantinos Vougioukas, Stavros Petridis, and Maja Pantic. End-to-end speech-driven facial animation with temporal gans. *ArXiv*, abs/1805.09313, 2018. 6

[72] Konstantinos Vougioukas, Stavros Petridis, and Maja Pantic. Realistic speech-driven facial animation with gans. *International Journal of Computer Vision*, 128(5):1398–1413, 2020. 1, 2, 3, 6

[73] Suzhen Wang, Lincheng Li, Yu Ding, Changjie Fan, and Xin Yu. Audio2head: Audio-driven one-shot talking-head generation with natural head motion. *arXiv preprint arXiv:2107.09293*, 2021. 2

[74] Zhou Wang, Alan C Bovik, Hamid R Sheikh, and Eero P Simoncelli. Image quality assessment: from error visibility to structural similarity. *IEEE transactions on image processing*, 13(4):600–612, 2004. 7

[75] Xin Wen, Miao Wang, Christian Richardt, Ze-Yin Chen, and Shi-Min Hu. Photorealistic audio-driven video portraits. *IEEE Transactions on Visualization and Computer Graphics*, 26(12):3457–3466, 2020. 2

[76] Haozhe Wu, Jia Jia, Haoyu Wang, Yishun Dou, Chao Duan, and Qingshan Deng. Imitating arbitrary talking style for realistic audio-driven talking face synthesis. In *Proceedings of the 29th ACM International Conference on Multimedia*, pages 1478–1486, 2021. 2

[77] Zhisheng Xiao, Karsten Kreis, and Arash Vahdat. Tackling the generative learning trilemma with denoising diffusion gans. *arXiv preprint arXiv:2112.07804*, 2021. 3

[78] Dongchao Yang, Jianwei Yu, Helin Wang, Wen Wang, Chao Weng, Yuexian Zou, and Dong Yu. Diffsound: Discrete diffusion model for text-to-sound generation. *arXiv preprint arXiv:2207.09983*, 2022. 3

[79] Ling Yang, Zhilong Zhang, Yang Song, Shenda Hong, Runsheng Xu, Yue Zhao, Yingxia Shao, Wentao Zhang, Bin Cui, and Ming-Hsuan Yang. Diffusion models: A comprehensive survey of methods and applications. *arXiv preprint arXiv:2209.00796*, 2022. 3

[80] Ruihan Yang, Prakhar Srivastava, and Stephan Mandt. Diffusion probabilistic modeling for video generation. *arXiv preprint arXiv:2203.09481*, 2022. 3

[81] Ran Yi, Zipeng Ye, Juyong Zhang, Hujun Bao, and Yong-Jin Liu. Audio-driven talking face video generation with learning-based personalized head pose. *arXiv preprint arXiv:2002.10137*, 2020. 2

[82] Chenxu Zhang, Yifan Zhao, Yifei Huang, Ming Zeng, Saifeng Ni, Madhukar Budagavi, and Xiaohu Guo. Facial: Synthesizing dynamic talking face with implicit attribute learning. In *Proceedings of the IEEE/CVF international conference on computer vision*, pages 3867–3876, 2021. 2

[83] Mingyuan Zhang, Zhongang Cai, Liang Pan, Fangzhou Hong, Xinying Guo, Lei Yang, and Ziwei Liu. Motiondiffuse: Text-driven human motion generation with diffusion model. *arXiv preprint arXiv:2208.15001*, 2022. 3

[84] Zhimeng Zhang, Lincheng Li, Yu Ding, and Changjie Fan. Flow-guided one-shot talking face generation with a high-resolution audio-visual dataset. In *Proceedings of the IEEE/CVF Conference on Computer Vision and Pattern Recognition*, pages 3661–3670, 2021. 2

[85] Ruiqi Zhao, Tianyi Wu, and Guodong Guo. Sparse to dense motion transfer for face image animation. In *Proceedings of the IEEE/CVF International Conference on Computer Vision*, pages 1991–2000, 2021. 1

[86] Hang Zhou, Yu Liu, Ziwei Liu, Ping Luo, and Xiaogang Wang. Talking face generation by adversarially disentangled audio-visual representation. In *Proceedings of the AAAI conference on artificial intelligence*, volume 33, pages 9299–9306, 2019. 3

[87] Hang Zhou, Yasheng Sun, Wayne Wu, Chen Change Loy, Xiaogang Wang, and Ziwei Liu. Pose-controllable talking face generation by implicitly modularized audio-visual representation. In *Proceedings of the IEEE/CVF conference on computer vision and pattern recognition*, pages 4176–4186, 2021. 1, 3, 6

[88] Yang Zhou, Xintong Han, Eli Shechtman, Jose Echevarria, Evangelos Kalogerakis, and Dingzeyu Li. Makelttalk: speaker-aware talking-head animation. *ACM Transactions on Graphics (TOG)*, 39(6):1–15, 2020. 1, 2, 6

[89] Hao Zhu, Huaibo Huang, Yi Li, Aihua Zheng, and Ran He. Arbitrary talking face generation via attentional audio-visual coherence learning. In *Proceedings of the Twenty-Ninth International Conference on International Joint Conferences on Artificial Intelligence*, pages 2362–2368, 2021. 3

[90] Jun-Yan Zhu, Taesung Park, Phillip Isola, and Alexei A Efros. Unpaired image-to-image translation using cycle-consistent adversarial networks. In *Proceedings of the IEEE international conference on computer vision*, pages 2223–2232, 2017. 2